Lateral flight control design for a highly flexible aircraft using nonsmooth optimization

Alberto M. Simões [*]
ONERA, Toulouse, France

Pierre Apkarian [†]
ONERA & UPS, Toulouse, France

Daniel Alazard [‡]
Université de Toulouse-ISAE, France

Dominikus Noll [§]
Université Paul Sabatier, Toulouse, France

This paper describes a nonsmooth optimization technique allowing to design a lateral flight control law for a highly flexible aircraft. Flexible modes and high-dimensional models pose a major challenge to modern control design tools. It is shown that the nonsmooth approach offers potent and flexible alternatives in this difficult context. More specifically, the proposed technique is used to achieve a mix of frequency domain as well as time domain requirements for a set of different load conditions.

I. Introduction

The synthesis of flight control laws for modern aeronautics and space applications remains a challenging task whenever aeroservoelastic phenomena significantly affect the control bandwidth. Such phenomena are especially critical when demanding specifications including performance and robustness constraints of different natures must be achieved. Performance specifications, for instance, are normally related to control objectives like tracking and decoupling and are naturally expressed in terms of time-domain constraints such as limited overshoot, short settling- or rise-times, small steady-state error and amplitude limitation. Flexible modes, on the other hand, are frequently dealt with via frequency-domain criteria or modal specifications (prescribed damping ratios). A further complication is related to

[*]Researcher, Control Systems Department.
[†]Researcher & Professor, Control Systems Department & Institut de Mathématiques.
[‡]Professor, Department of Mathematics, Computer and Control Sciences.
[§]Professor, Institut de Mathématiques.

structural constraints imposed on the controller. Simpler controllers are generally sought to facilitate on-board implementation and management.

The classical approach in which a control law is designed for the rigid dynamics and a low-pass filter is inserted a posteriori to avoid or reduce spillover effects is no longer a valid scheme for such applications. The reason is that in order to meet appropriate level of performance, the controller bandwidth should overlap with the frequency range of flexible modes which represents a core issue of such problems.

Traditional H_2 or H_∞ syntheses[20] do not provide suitable answers to these difficulties. First of all, time-domain specifications should be addressed indirectly via nontrivial tuning of weighting filters. Secondly, these methods produce full-order controllers and therefore rely on model reduction techniques to derive simple controllers which is always prone to failure.

Design methods based on the Youla parametrization[8] offer some flexibility to handle both time- and frequency-domain specifications. The resulting controllers however suffer from substantial order inflation and are hardly amenable to numerical implementation.

Different approaches have been reported in the literature trying to exploit eigenstructure assignment methods to design problems involving lightly-damped flexible modes.[13,14,17] Eigenstructure assignment methods are interesting because time-domain specifications can be captured through modal shaping. Unfortunately, as noted in Ref. 13, determining appropriate eigenspaces associated with flexible modes remains an inherent difficulty.

Nonsmooth optimization techniques have been used recently to solve a number of difficult structured controller design problems involving time- or frequency-domain specifications.[2,3,7,9,12,18] The nonsmooth design method considered here bear the following appealing features. First, time-domain specifications are addressed directly, thus dispensing with the use of auxiliary tuning parameters such as weighting filters. Moreover, frequency-domain constraints such as those related to flexible modes are easily incorporated within the same framework. Secondly, such techniques remain operational even for large size plants, and thus allow to short-circuit risky model reduction phases. Finally, they encompass arbitrary controller structures which make them methods of choice when implementation constraints are important.

The central aim of the present work is to illustrate the efficiency and the flexibility of nonsmooth design methods in solving difficult structured control design problems like large size flexible transport aircraft.

The paper is organized as follows. Section II discusses the multi-objective control design problem, while Section III outlines the key ingredients of the proposed nonsmooth optimization technique. The difficult design problem of lateral flight control for a highly flexible aircraft subject to turbulence and multiple load conditions is addressed in Section IV.

II. Multi-objective controller design via nonsmooth optimization

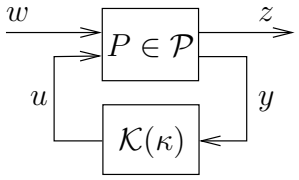

Figure 1. Closed-loop synthesis interconnection

To begin with, consider the synthesis interconnection given by the standard form in Fig. 1 with $u \in \mathbb{R}^{m_2}$ and $y \in \mathbb{R}^{p_2}$ and where the multivalued plant $P(s)$ takes values in a finite family of linear plants $\mathcal{P} := \{P^1, \ldots, P^p\}$ representing, for instance, multiple operating conditions or faulty modes. Each plant $P \in \mathcal{P}$ is described by a minimal state-space realization of the form

$$\begin{bmatrix} \dot{x}(t) \\ z(t) \\ y(t) \end{bmatrix} = \begin{bmatrix} A & B_1 & B_2 \\ C_1 & D_{11} & D_{12} \\ C_2 & D_{21} & D_{22} \end{bmatrix} \begin{bmatrix} x(t) \\ w(t) \\ u(t) \end{bmatrix}, \tag{1}$$

where plant indexing has been removed for simplicity. In order to address practical controller structures we introduce a state-space parametrization of the form

$$\kappa \in \mathbb{R}^q \to \mathcal{K}(\kappa) := \begin{bmatrix} A_K(\kappa) & B_K(\kappa) \\ C_K(\kappa) & D_K(\kappa) \end{bmatrix} \tag{2}$$

with corresponding frequency-domain representation

$$K(s, \kappa) = C_K(\kappa)(sI - A_K(\kappa))^{-1} B_K(\kappa) + D_K(\kappa),$$

where $A_K \in \mathbb{R}^{k \times k}$. In the above description, κ designates the decision vector of design variables in the controller. Note the case of a static controller ($k = 0$) is a particular instance. The mapping $\mathcal{K}: \mathbb{R}^q \to \mathbb{R}^{(m_2+k)\times(p_2+k)}$ is assumed to be continuously differentiable but otherwise arbitrary.

Performance specifications are given in most cases in terms of time-domain constraints like limited overshoot, short settling- or rise-times, but also amplitude limitation in order to guarantee decoupling properties or to avoid reaching operational limits of the system. Such time-domain constraints are achieved by direct shaping closed-loop system responses to fixed test input signals. More specifically, it is assumed that each plant in the family $\mathcal{P}$ in feedback loop with the controller $K(s, \kappa)$ is subject to one or several input signals w selected in a finite signal generator set $\mathcal{W} := \{w^1, \ldots, w^d\}$. This gives rise to a finite family

of closed-loop responses $z \in \mathcal{Z}$, where $\mathcal{Z} := \{z^1, \ldots, z^r\}$. Each instance in $\mathcal{Z}$ is called a scenario. Practically speaking, the signal generator set is made of typical deterministic test inputs such as steps, ramps, sinusoids, etc.

The above description is flexible enough to reflect situations in which a single plant is submitted to various test signals as in the case when decoupling properties must be examined, or when the response to a given test signal is to be considered for multiple operating conditions or faulty modes. The proposed set-up also accepts more complicate formulations where each plant in the family $\mathcal{P}$ is tested against several inputs.

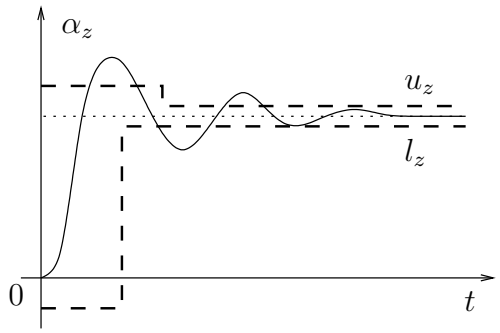

Figure 2. Envelope constraints on the step response

The goal is to compute $\kappa \in \mathbb{R}^q$ such that the closed-loop time responses $z \in \mathcal{Z}$ obtained with controller $\mathcal{K}(\kappa)$ meet envelope constraints of the form

$$l_z(t) \leq z(t) \leq u_z(t),\ \forall t \geq 0,\ \forall z \in \mathcal{Z}, \tag{3}$$

where l_z and u_z are lower and upper bounds for z and are assumed piecewise constant in the sequel. These bounds are illustrated as dashed lines in Fig. 2 for a step following specification (α_z stands for a coordinate of z).

On the other hand, design specifications including attenuation of exogenous bounded-energy disturbances or robustness against unstructured uncertainties are known to be better addressed by frequency-domain criteria involving bounds on the maximum singular value norm of suitable closed-loop transfers. Therefore, in addition to the constraints in (3), the designed controller $\mathcal{K}(\kappa)$ is required to achieve prescribed bounds for a finite set of closed-loop transfers

$$\|\mathcal{F}_l\left(P(s), K(s,\kappa)\right)\|_{I_P} \leq \gamma_P,\ \gamma_P > 0,\ \forall P \in \mathcal{P}^\infty \subset \mathcal{P}, \tag{4}$$

where $\mathcal{F}_l(\cdot,\cdot)$ denotes the traditional lower Linear Fractional Transformation, and $\|.\|_{I_P}$ denotes the peak value of the transfer function maximum singular value norm on a prescribed

frequency interval I_P:

$$\|\mathcal{F}_l\left(P(s),K(s,\kappa)\right)\|_{I_P} := \sup_{\omega\in I_P} \overline{\sigma}\left(\mathcal{F}_l\left(P(j\omega),K(j\omega,\kappa)\right)\right).$$

The frequency band I_P is typically a closed interval $I_P = [\omega_1^P, \omega_2^P]$, or more generally, a finite union of intervals $I_P = [\omega_1^P, \omega_2^P] \cup \ldots \cup [\omega_q^P, \omega_{q+1}^P]$, where right interval tips may take infinite values. Alternatively, a dynamic weight $W_P(s)$ can be included in (4) if necessary

$$\|W_P(s)\mathcal{F}_l\left(P(s),K(s,\kappa)\right)\|_{I_P} \leq 1,\ \forall P \in \mathcal{P}^\infty \subset \mathcal{P} \tag{5}$$

to stress the relative importance of each channel.

Finally, the most fundamental specification for a closed-loop system is internal stability. Thus, the sought controller $\mathcal{K}(\kappa)$ must also guarantee negative upper bounds on the closed-loop spectral abscissas (maximum real part of closed-loop eigenvalues)

$$\alpha(\mathcal{A}_P(\kappa)) \leq \alpha_P,\ \alpha_P < 0,\ \forall P \in \mathcal{P}, \tag{6}$$

where $\mathcal{A}_P(\kappa)$ is the state matrix of the closed-loop system $\mathcal{F}_l\left(P(s),K(s,\kappa)\right)$.

In summary, the considered multi-objective controller design problem may be stated as: find controller variables $\kappa \in \mathbb{R}^q$ such that constraints (3)-(6) are satisfied. In what follows this problem is addressed through a nonsmooth optimization technique. Notice, initially, that the time-domain constraints in (3) are automatically met if the function

$$f_t(\kappa) := \max_{z\in\mathcal{Z}} \max_{t\geq 0} \left\{[z(\kappa,t) - u_z(t)]_+,\ [l_z(t) - z(\kappa,t)]_+\right\} \tag{7}$$

is non-positive, where the notation $[.]_+$ applied to a vector $v \in \mathbb{R}^n$ is defined as $[v]_+ = \max\{0, \max_{i=1,\ldots,n} v_i\}$. Similarly, the frequency-domain constraints in (4) and the spectral constraints in (6) are satisfied if the functions

$$f_\infty(\kappa) := \max_{P\in\mathcal{P}^\infty} \frac{\|\mathcal{F}_l\left(P(s),K(s,\kappa)\right)\|_{I_P}}{\gamma_P} - 1 \tag{8}$$

and

$$g_\alpha(\kappa) := \max_{P\in\mathcal{P}} \left(\alpha(\mathcal{A}_P(\kappa)) - \alpha_P\right), \tag{9}$$

are non-positive, respectively.

Our nonsmooth design method is thus based on solving the max-type optimization prob-

lem

$$\begin{aligned} \underset{\kappa\in\mathbb{R}^q}{\text{minimize}} \quad & f(\kappa) := \max\{f_t(\kappa), f_\infty(\kappa)\} \\ \text{subject to} \quad & g_\alpha(\kappa) \leq 0\,. \end{aligned} \tag{10}$$

Note that a feasible solution κ^* to (10) also solves the original multi-objective design problem whenever the final objective value $f(\kappa^*)$ is non-positive. Program (10) is nonconvex, nonsmooth and semi-infinite, and therefore represents a challenging mathematical programming problem. Instead of using alternative smooth formulations which can be very expansive computationally (see Ref. 15 for an example), a specialized nonsmooth optimization technique with global convergence properties and allowing to solve (10) directly has been developed in Ref. 3. Global convergence refers here to the convergence towards a locally optimal solution from an arbitrary, even remote, starting point. In case $f(\kappa^*)$ is positive, a restart with a different seed will be required if the specifications set (3)-(6) are to be kept unchanged because the proposed technique only provides local solutions.

Program (10) can be seen as a Chebyshev norm-based scalarization of the original multi-objective design problem in which the role of individual weights for the various specifications is played by the tuning parameters l_z, u_z, γ_P and α_P. The strategy adopted here to select these weights is close in spirit to the aspiration levels approach for multi-objective optimization [8, p.64]. The tuning parameters are then adjusted iteratively based on a few trial-and-error designs: satisfied constraints can be strengthened while violated constraints can be relaxed. Indeed, one of the appealing features of the present design method is that tuning parameters are closely related to engineering specifications, so that their adjustment is fairly straightforward.

The design framework described by program (10) and the nonsmooth optimization technique discussed below is flexible enough to accommodate an even richer set of specifications. The reader is referred to Ref. 4 for further examples. At this stage it is important to emphasize that program (10) does not involve any Lyapunov variables as would be the case if LMI formulations were used. The size of such variables grows quadratically with the plant dimension which is a major impediment for application to realistic problems. As we shall see later the proposed nonsmooth method remains at ease even for high-order plants.

III. Nonsmooth optimization technique

In this section, the key ingredients of the nonsmooth optimization technique are briefly presented. Proofs for the main results are available in Refs. 2, 3.

Initially, a strictly feasible point for program (10) is found using the results in Ref. 6. For α_P close to zero in (9), this is essentially equivalent to finding a controller $K(s,\kappa)$ that simultaneously stabilizes in closed-loop all the models in $\mathcal{P}$. Next, program (10) is solved

based on a simplified form of the progress function introduced by Polak:[16]

$$F(\kappa^+, \kappa) = \max\{f(\kappa^+) - f(\kappa); g_\alpha(\kappa^+)\}, \tag{11}$$

where κ represents the current iterate and κ^+ the next iterate or a candidate to become the next iterate.

The key fact about the progress function (11) is that a critical point κ^* of $F(\cdot, \kappa^*)$ will also be a critical point of the original program (10).[3,16] A critical point κ^* of $F(\cdot, \kappa^*)$ is a point such that $0 \in \partial_1 F(\kappa^*, \kappa^*)$, where $\partial_1 F(\kappa^*, \kappa^*)$ denotes the Clarke subdifferential[10] of $F(\cdot, \kappa^*)$ with respect to the first variable at κ^*. The following iterative procedure is used to determine such a point. Suppose the current iterate κ is such that $0 \notin \partial_1 F(\kappa, \kappa)$, which implies that it is possible to reduce the function $F(\cdot, \kappa)$ in a neighborhood of κ, that is, to find κ^+ such that $F(\kappa^+, \kappa) < F(\kappa, \kappa)$. Replacing κ by κ^+, the procedure is repeated. Unless $0 \in \partial_1 F(\kappa^+, \kappa^+)$, in which case a critical point has been attained, it is possible again to find κ^{++} such that $F(\kappa^{++}, \kappa^+) < F(\kappa^+, \kappa^+)$, etc. The sequence $\kappa, \kappa^+, \kappa^{++}, \ldots$ so generated is expected to converge to the sought local minimum κ^* of (10).

The initial κ being strictly feasible, all consecutive iterates will remain inside the feasibility region and, consequently, inside the stability region. To realize that, notice that $F(\kappa, \kappa) = 0$, so the left hand term in (11) is active at κ. Since the new κ^+ is such that $F(\kappa^+, \kappa) < F(\kappa, \kappa) = 0$, one necessarily has $g(\kappa^+) \leq F(\kappa^+, \kappa) < 0$, which means that κ^+ is also strictly feasible. Moreover, this also means that the objective is minimized, since $f(\kappa^+) - f(\kappa) \leq F(\kappa^+, \kappa) < 0$. By forcing iterates to remain in the stability region, one guarantees that the algorithm will progress in a region where function f_∞ in (8) is well defined.

The descent step κ^+ away from the current κ is found using a first-order estimate of a local minimizer for $F(\cdot, \kappa)$. To that end, a first-order convex approximation $\widehat{F}(\cdot, \kappa)$ of $F(\cdot, \kappa)$ around κ is built, and the following program is solved at κ:

$$\underset{d\kappa \in \mathbb{R}^q}{\text{minimize}}\ \widehat{F}(\kappa + d\kappa, \kappa) + \tfrac{\delta}{2} \|d\kappa\|^2, \quad \delta > 0\,. \tag{12}$$

Let $d\kappa$ denote the solution of the tangent program (12). Then $\kappa + d\kappa$ represents a first-order estimate of a local minimizer for $F(\cdot, \kappa)$. In particular, $d\kappa$ provides a descent direction for the progress function $F(\cdot, \kappa)$ at κ. The next iterate is then $\kappa^+ = \kappa + d\kappa$, or possibly $\kappa^+ = \kappa + \rho d\kappa$ for a suitable stepsize $\rho \in (0, 1)$ found by an Armijo backtracking line search[11] and such that

$$F(\kappa + \rho d\kappa, \kappa) - F(\kappa, \kappa) \leq \zeta \rho F^o(\kappa, d\kappa) < 0, \tag{13}$$

where $0 < \zeta < 1$ and $F^\circ(\kappa, d\kappa)$ denotes the generalized directional derivative of $F(\cdot, \kappa)$ at κ

in the direction $d\kappa$. The Armijo condition guarantees global convergence of the algorithm to a F. John[16] point which is a local minimum in general. Finally, $0 \in \partial_1 F(\kappa, \kappa)$ if $d\kappa = 0$, so $d\kappa = 0$ is a necessary optimality condition for the original program (10) which may be used in practice as a stopping criterion.

The nonsmooth algorithm may be summarized as follows:

Algorithm 1 Nonsmooth algorithm for program (10)

Parameters: $\delta > 0$, $0 < \beta, \zeta < 1$.

1: **Initialize**. Choose closed-loop stabilizing κ

2: **Stopping test**. If $0 \in \partial_1 \widehat{F}(\kappa, \kappa)$ then stop. Otherwise continue.

3: **Compute descent direction.** Solve tangent program (12)

$$\min_{d\kappa} \widehat{F}(\kappa + d\kappa, \kappa) + \frac{\delta}{2}\|d\kappa\|^2.$$

Solution is the search direction $d\kappa$.

4: **Line search.** Find $\rho = \beta^\nu$, $\nu \in \mathbb{N}$, satisfying the Armijo condition

$$F(\kappa + \rho d\kappa, \kappa) - F(\kappa, \kappa) \leq \zeta \rho F^o(\kappa, d\kappa) < 0.$$

5: **Update**. Put $\kappa \leftarrow \kappa + \rho d\kappa$. Loop back to step 2.

In order to build the first-order approximation $\widehat{F}(\cdot, \kappa)$ of $F(\cdot, \kappa)$ used in (12), one need initially to gather first-order information on the various specifications represented by f_t, f_∞ and g_α. For the spectral abscissa specification in g_α, the subdifferential of the function $\partial(\alpha \circ \mathcal{A}_P)(\kappa)$ has been given in Ref. 6. Subgradients computation involves only basic linear algebra operations and therefore can be performed very efficiently. The subdifferential of the maximum singular value norm appearing in f_∞ shares a similar structure.[2,18] Finally, subgradients computation for f_t relies on closed-loop simulations which can be performed very efficiently for LTI systems.[7] With these preparations, program (12) can be equivalently formulated as a standard convex quadratic program (CQP), which can be efficiently solved using currently available state-of-the-art codes. The quadratic term in (12) can be used to capture second-order information or may be interpreted as a trust region radius management parameter.

IV. Application to lateral flight control design of a highly flexible aircraft

Problem description

The nonsmooth method outlined above is used in this section to design a flight controller for the lateral motion of a large carrier aircraft in which flexibility has been intentionally degraded to a highly critical level in order to build a difficult control problem and to test the efficiency of various modern techniques. It is a realistic challenging problem which has been initially presented in Ref. 1.

The design specifications for this application are particularly tight. Besides good-handling qualities in time domain, the flight controller must also achieve improved comfort during turbulence despite the presence of lightly-damped flexible modes. An additional difficulty here is that the location of the flexible modes in the complex plane changes with the distribution of the mass inside the plane, as one can notice by comparing both loci depicted in Fig. 8. Consequently, the closed-loop system must also be robust with respect to changes in the load condition.

Six linearized models of the lateral motion of the aircraft around equilibrium points are considered here. They correspond to six distributions of the mass inside the plane under the same flight condition. Each model is described by a **68^{th}-order** state-space representation whose state vector contains 4 rigid states (yaw angle β, roll rate p, yaw rate r and roll angle ϕ), 36 states corresponding to 18 flexible modes, 20 secondary states representing the dynamics of servocontrol surfaces and aerodynamic lags, and 8 states modeling turbulence as exogenous disturbance. There are two control inputs, aileron deflection δ_l and rudder deflection δ_n, and one exogenous disturbance input v representing gusts.

For the sake of comparison, the same six measurements used in Ref. 1 are also used here, which are the roll rate p_6 and angle ϕ_6 measured at the center of the plane, the yaw rates r_1 and r_{11} at the front and the rear of the aircraft, respectively, and the lateral accelerations n_{y7} and n_{y9} measured at two different points of the fuselage (11 location points are regularly spaced from 1 at the front to 11 at the rear of the fuselage). This set of measurements was selected according to observability properties of the rigid model and first flexible modes (in an increasing order of pulsation) with respect to sensors location along the fuselage.

The design specifications defined for this problem can then be summarized as follows:

[S1] flying quality requirements materialized by time-domain templates on the step responses with respect to β and ϕ,

[S2] large Dutch roll damping ratio,

[S3] no degradation, or preferably improvement in damping ratios of flexible modes,

[S4] improved comfort during turbulence. The comfort performance index is measured on the frequency response of transfers between the gust v and lateral accelerations at the front n_{y1}, the middle n_{y6} and the rear n_{y11} of the fuselage,

[S5] robustness with respect to the various loading conditions,

[S6] to facilitate on-board implementation a reduced-order controller order is desirable.

Nonsmooth synthesis

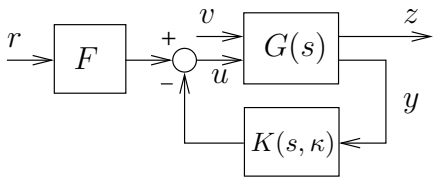

Figure 3. closed-loop interconnection for flexible aircraft

The adopted control configuration and the corresponding synthesis interconnection are depicted in Fig. 3, where $G(s)$ represents the aircraft transfer matrix for a given load condition, $u = [\,\delta_l \quad \delta_n\,]^T$ is the control input, $y = [\,n_{y7} \quad n_{y9} \quad p_6 \quad r_1 \quad r_{11} \quad \phi_6\,]^T$ is the measured output and $r := [\,\beta_r \quad \phi_r\,]^T$ is the reference vector. Different outputs will be selected so as to form the regulated output vector z according to the various criteria.

Using the flexibility provided by parametrization (2), the feedback controller $K(s,\kappa)$ is chosen as a 10^{th}-order state-space system, thereby ensuring controller simplicity as required by specification [S6]. For comparison, it should be noticed that the least controller order achieved in Ref. 1 using model reduction techniques was 20. Additionally, the feedback controller is forced to be strictly proper ($D_K(\kappa) \equiv 0$ in (2)) in order to improve robustness with respect to high frequency flexible modes and to achieve better noise attenuation. The feedforward controller $F \in \mathbb{R}^{2\times 2}$ is selected as a static matrix gain to facilitate implementation.

The first time-domain specification in [S1] imposed on the final closed-loop system is the steady-state constraint

$$\lim_{t\to\infty} \begin{bmatrix} \beta(t) \\ \phi(t) \end{bmatrix} = \begin{bmatrix} 1 & 0 \\ -1 & 1 \end{bmatrix} \lim_{t\to\infty} \begin{bmatrix} \beta_r(t) \\ \phi_r(t) \end{bmatrix}. \tag{14}$$

This constraint can be addressed through appropriate selection of the pre-filter gain F.

Notice that in accordance to the final value theorem, (14) implies that

$$\mathcal{F}_l\left(G_{\beta\phi}(0), -K(0,\kappa)\right) F = \begin{bmatrix} 1 & 0 \\ -1 & 1 \end{bmatrix}, \tag{15}$$

where $G_{\beta\phi}(s)$ is the open-loop transfer matrix from $[\, u^T \quad u^T \,]^T$ to $[\, [\, \beta \quad \phi \,] \quad y^T \,]^T$. Therefore, (14) will be automatically met if F is derived through

$$F = \mathcal{F}_l\left(G_{\beta\phi}(0), -K(0,\kappa)\right)^{-1} \begin{bmatrix} 1 & 0 \\ -1 & 1 \end{bmatrix}, \tag{16}$$

assuming existence of the inverse matrix. In practice, (16) can be written equivalently as

$$F = \mathcal{F}_l\left(M, K(0,\kappa)\right) \begin{bmatrix} 1 & 0 \\ -1 & 1 \end{bmatrix}, \tag{17}$$

where matrix M is such that

$$\mathcal{F}_l\left(M, K(0,\kappa)\right) = \mathcal{F}_l\left(G_{\beta\phi}(0), -K(0,\kappa)\right)^{-1},$$

Existence of matrix M is guaranteed by the fact that the open-loop transfer matrix from u to $[\, \beta \quad \phi \,]$ is non-singular.[20] The feedforward gain F is thus uniquely determined by the design variables vector κ via the continuously differentiable parametrization (17), which can be easily incorporated into the proposed nonsmooth method. Consequently, both feedback and feedfoward controllers will be designed simultaneously by the nonsmooth technique.

As discussed in Section II, the time-domain templates translating flying quality requirements in [S1] are handled directly within the nonsmooth method. Two basic scenarios are initially considered. In the first scenario, a unit step is applied to reference β_r while v and ϕ_r are considered to be zero, and appropriate envelope constraints are imposed on the relevant outputs. Fig. 4 depicts the envelope constraints imposed on rigid β and ϕ for this scenario, as well as the evolution of the system responses throughout the optimization sequence, starting from the initial stabilizing controller. Notice that constraints such as minimal phase response for ϕ can be addressed easily via time-domain templates. The second scenario consists in a unit step being applied to ϕ_r while the other two inputs are kept to zero. The corresponding envelope constraints imposed on rigid β and ϕ are depicted in Fig. 5.

In order to improve performance robustness with respect to load variation, as required by [S5], the above scenarios are considered for two extreme load conditions: the lightest and the heaviest models. In the framework of Section II, this means that the plant family $\mathcal{P}$ will consist of two models which we refer to by light and heavy. Correspondingly, two different test inputs as discussed previously will be applied to both plants. This results in a total of

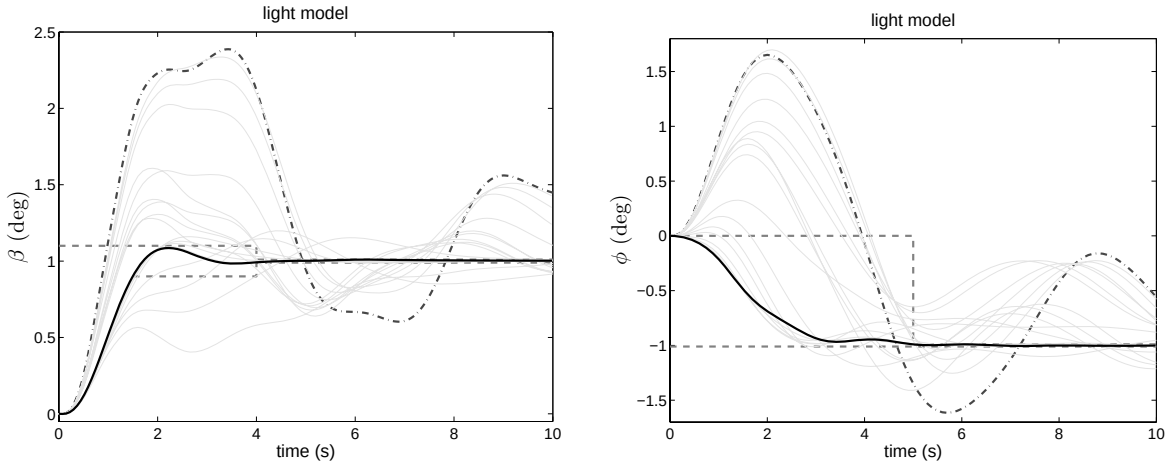

Figure 4. Evolution of closed-loop β_r step responses (dashed: initial stabilizing controller, solid: final controller)

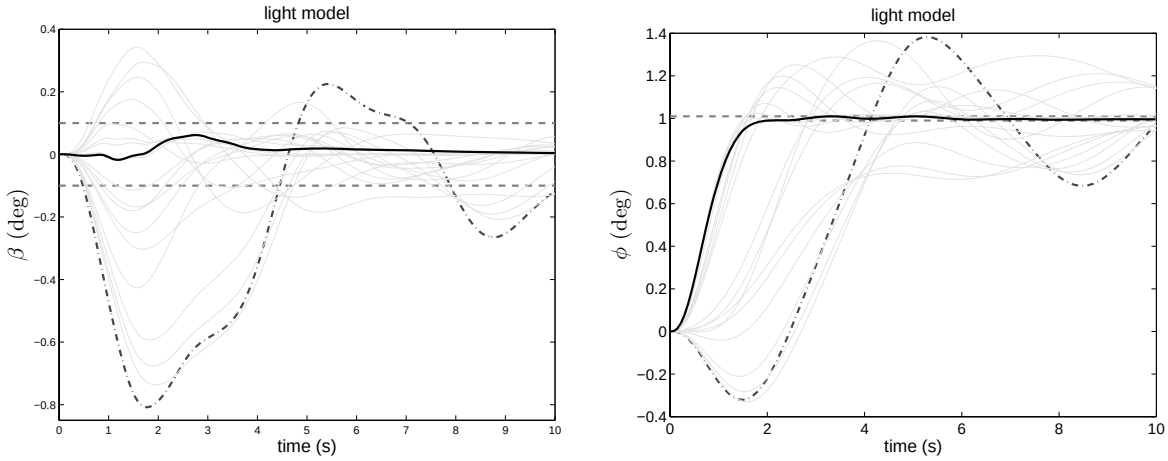

Figure 5. Evolution of closed-loop ϕ_r step responses (dashed: initial stabilizing controller, solid: final controller)

four scenarios which must be adequately controlled. The main idea here is that by ensuring similar system responses even under extreme load variations, satisfactory closed-loop system behavior can also be expected for intermediate conditions. If, however, final closed-loop system response proves to be unsatisfactory for a given intermediate load condition, one may alternatively restart the design but this time taking the critical intermediate scenario into account via an enriched plant family $\mathcal{P}$. Analogously, constraints are imposed via (9) on the closed-loop spectral abscissas with both light and heavy models to achieve stability robustness requirements.

The feedforward gain F is not dependent on load conditions, so a nominal model has to be defined in (16): the light model has been selected to play this role. Notice, however, that

the case of an adaptive gain could also be easily handled: the only change necessary would be to consider in (16) the transfers $G_{\beta\phi}$ accordingly.

Improvement in comfort during turbulence is obtained by minimizing, in the flexible modes frequency range, the magnitude of the transfer functions from the exogenous disturbance v to the lateral acceleration measured at three distinct points of the fuselage: front (n_{y1}), center (n_{y6}) and rear (n_{y11}). Fig. 6 shows the corresponding transfer magnitudes for the uncontrolled plant and the corresponding achieved closed-loop frequency responses. Horizontal dashed lines in Fig. 6 materialize bounds which have been prescribed via γ_P in (8). These frequency-domain constraints have been defined for both light and heavy models in order to improve robustness with respect to load variations.

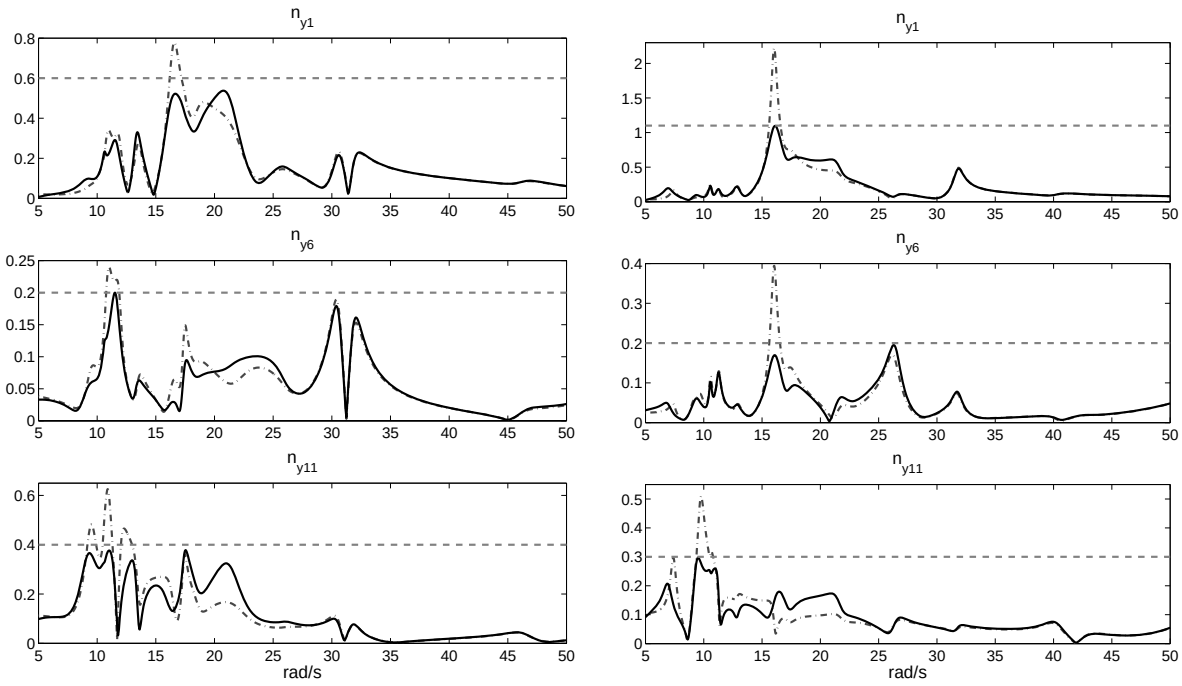

(a) light (b) heavy

Figure 6. Magnitudes of the transfers from v to lateral accelerations (dashdot: open-loop plant, solid: final closed-loop)

Finally, norm constraints (5) are imposed on the sensibility function $S = (I + G_y K)^{-1}$, $G_y(s)$ being the open-loop transfer from u to y, for both light and heavy models. In addition to increasing the stability margin, these constraints allows to increase the damping ratios of the Dutch roll and the flexible modes. The largest singular-value of S is depicted in Fig. 7 for both light and heavy loads. The dashed-lines in Fig. 7 represent the corresponding desired norm-bounds defined via dynamic weights W_P in (5).

It is well-known that pole-zero cancellations is a critical issue when designing controllers with frequency domain techniques. Incorporating various load conditions in the synthesis is

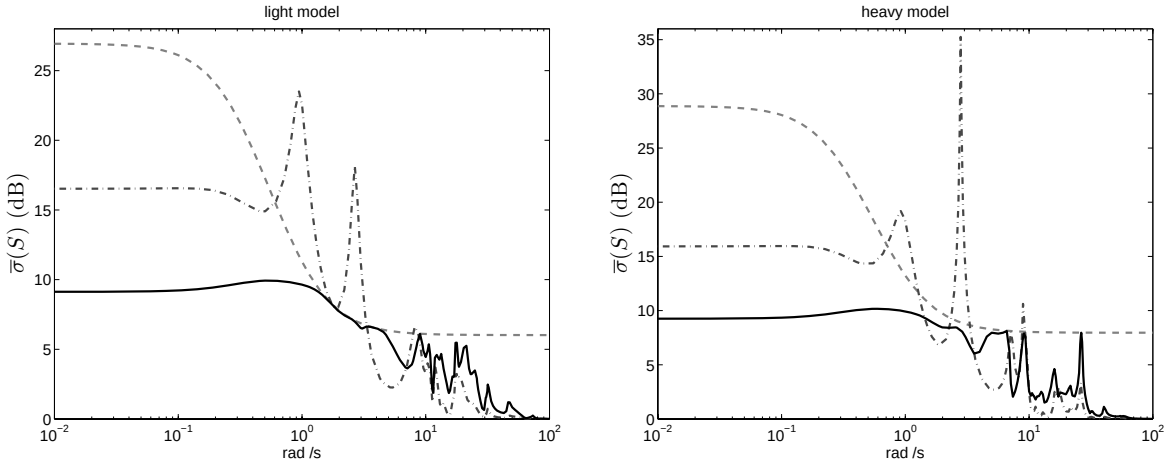

Figure 7. Largest singular-value of the sensibility function (dashdot: initial stabilizing controller, solid: final controller) and W_P^{-1}(dash)

a simple device to overcome cancellations of flexible modes. In the same vein, the possibility to work with low-order controllers (order 10 as compared to the plant order of 68) is another favorable feature to prevent pole/zero cancellations. The H_2/PRLQG[19] criterion used in Ref. 1 to increase the damping ratios of flexible modes is another potential option which requires constructing a linear fractional representation to model parametric uncertainty in flexible modes. This route has not been followed here as LFT models suggest using μ-synthesis as design tool with the difficulties discussed above in terms of controller order and structure.

All computations and simulations have been performed within the Matlab environment. The nonsmooth algorithm has been developed in Matlab language, with Fortran being used for some key components like the CQP tangent program (12) in order to enhance computational performance. One of the main assets of the proposed design method is the possibility of integrating specifications directly as they appear in the design specifications, as it significantly facilitates tuning the specification weights. Indeed, only a few *optimization−weight adjustment* loops have been necessary in order to find a satisfactory solution. The nonsmooth algorithm required 432 iterations in 122 minutes on a 2.4GHz Core 2 Quad processor with 4Gb RAM to find the final controller at the last stage.

Fig. 8 depicts the position of closed-loop poles in the complex plane as the controller gain is varied from 0 to 100%. As required, the Dutch roll damping ratio has been significantly increased, as well as the damping ratios of the first flexible modes [a]. Additionally, no critical damping ratio degradation is observed.

Closed-loop system responses for six different load conditions are depicted in Fig. 9, more precisely the rigid yaw angle β together with the roll rate p_6, the yaw rate r_6 and

[a]The flexible mode at $0.146 \pm 10.6j$ is uncontrollable.

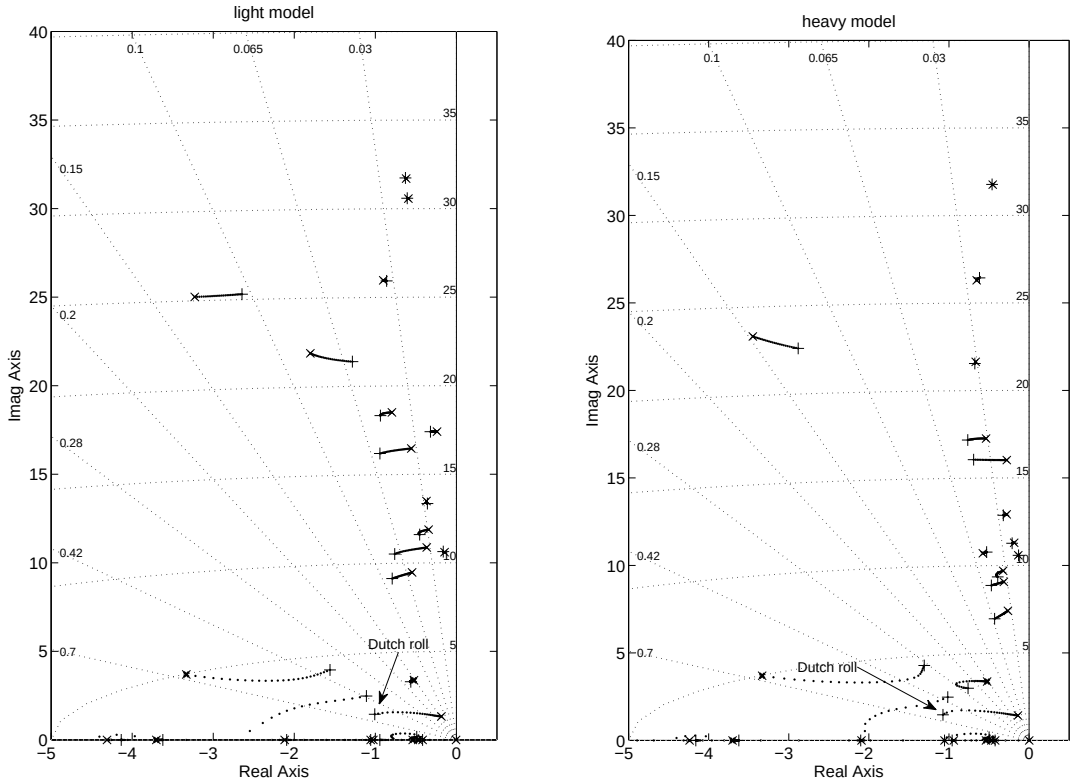

Figure 8. Root-locus analysis ('x': open-loop, '+':closed-loop)

the roll angle ϕ_6 measured at the center of the airplane. System responses meet the flying quality requirements and robust performance has been obtained. Additionally, the closed-loop system satisfies comfort and damping ratio requirements for all load conditions.

V. Conclusion

This paper has focused on the design of a flight controller for the lateral motion of a highly flexible aircraft subject to exogenous disturbances and different load conditions. A reduced-order feedback controller as well as a static feed-forward controller have been designed simultaneously without recourse to risky order reduction schemes. The study case is a challenging application as it involves a 68th-order plant, several operating conditions and stringent time- and frequency domain specifications in addition to structural constraints on the controller. The proposed nonsmooth optimization technique has been shown to hold promise in solving a set of concurrent constraints and in achieving turbulence attenuation and robustness with respect to flexible mode uncertainties.

The proposed approach is local in nature which means optimality certificates are local as opposed to the indisputable global certificate. As corroborated by the challenging applica-

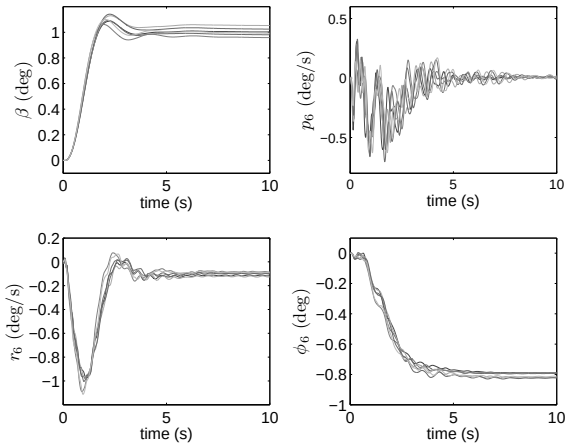

(a) β_r step response

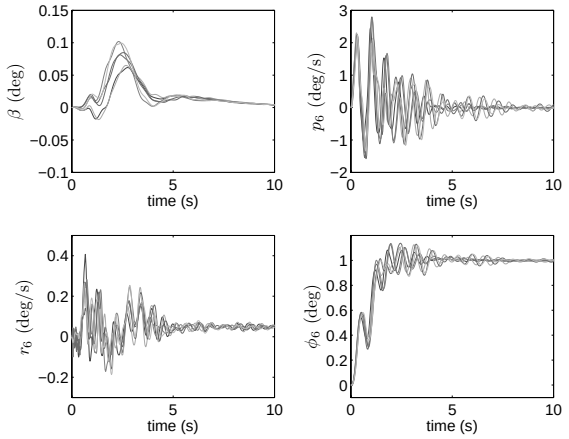

(b) ϕ_r step response

Figure 9. Closed-loop system responses under different load configurations

tion discussed here, this is a minor weakness widely offset by the flexibility to directly cope with multiple specifications. Specifications are indeed handled as stated in practice by designers thus bypassing conservative embeddings as is usually the case with more traditional techniques.

References

[1]D. Alazard. Robust H_2 design for lateral flight control of highly flexible aircraft. *AIAA J. of Guidance, Control, and Dynamics*, 25(3), 2002.

[2]P. Apkarian and D. Noll. Nonsmooth H_∞ synthesis. *IEEE Trans. Aut. Control*, 51(1):71–86, 2006.

[3]P. Apkarian, D. Noll, and A. Rondepierre. Mixed H_2/H_∞ control via nonsmooth optimization. *SIAM J. on Control and Optimization*, 47(3):1516–1546, 2008.

[4]P. Apkarian and D. Noll. IQC analysis and synthesis via nonsmooth optimization. *Syst. Control*

Letters, 55(12):971 – 981, 2006.

[5]G. J. Balas and J. C. Doyle. Control of lightly damped, flexible modes in the controller crossover region. *Journal of Guidance Control Dynamics*, 17:370–377, March 1994.

[6]V. Bompart, P. Apkarian, and D. Noll. Non-smooth techniques for stabilizing linear systems. *American Control Conference, 2007. ACC '07*, pages 1245–1250, July 2007.

[7]V. Bompart, P. Apkarian, and D. Noll. Control design in the time- and frequency-domain using nonsmooth techniques. *Syst. Control Letters*, 57(3):271–282, 2008.

[8]S. Boyd and C. Barratt. *Linear Controller Design: Limits of Performance*. Prentice-Hall, 1991.

[9]J. V. Burke, A. S. Lewis, and M. L. Overton. Robust Gradient Sampling Algorithm for Nonsmooth, Nonconvex Optimization. *SIAM J. Optimization*, 15(3):751–779, 2005.

[10]F. H. Clarke. *Optimization and Nonsmooth Analysis*. Canadian Math. Soc. Series. John Wiley & Sons, New York, 1983.

[11]Jr. J.E. Dennis and R.Schnabel. *Numerical methods for unconstrained optimization and nonlinear equations*. SIAM's Classics in Applied Mathematics. SIAM, 1996.

[12]S. Gumussoy and M. L. Overton. Fixed-order H_∞ controller design via HIFOO, a specialized nonsmooth optimization package. *American Control Conference, 2008*, pages 2750–2754, June 2008.

[13]F. Kubica, T. Livet, X. Le Tron, and A. Bucharles. Parameter-robust flight control system for a flexible aircraft. *Control Engineering Practice*, 3(9):1209 – 1215, 1995.

[14]M. Merkel, M. H. Gojny, and U. B. Carl. Enhanced eigenstructure assignment for aeroelastic control application. *Aerospace Science and Technology*, 8(6):533 – 543, 2004.

[15]Y. Piguet, U. Holmberg, and R. Longchamp. A minimax approach for multi-objective controller design using multiple models. *Int. J. Control*, 72(7):716–726, may 1999.

[16]E. Polak. *Optimization : Algorithms and Consistent Approximations*. Applied Mathematical Sciences, 1997.

[17]M. Sato and M. Suzuki. Vibration control of flexible structures using a combined H_∞ filter approach . *AIAA J. of Guidance, Control, and Dynamics*, 19(5):1000–1006, 1996.

[18]A. M. Simões, P. Apkarian, and D. Noll. A nonsmooth progress function for frequency shaping control design. *IET Control Theory & Applications*, 2(4):323–336, April 2008.

[19]M. Tahk and J. L. Speyer. Parameter robust linear-quadratic-Gaussian design synthesis with flexible structure control applications. *AIAA J. of Guidance, Control, and Dynamics*, 12:460–468, 1989.

[20]K. Zhou, J. C. Doyle, and K. Glover. *Robust and Optimal Control*. Printice Hall, 1996.